A multi-tissue segmentation of the human head for detailed computational models

Markus Hannula, Nathaniel Narra, Niina Onnela, Prasun Dastidar and Jari Hyttinen

***Abstract*—This paper describes the creation of an anatomically detailed high resolution model of the human head based on the Visible Human Female data from the National Library of Medicine archives. Automatic and semi-automatic segmentation algorithms were applied over the 3 image volumes – CT, MRI and anatomical cryo-sections of the cadaver – to label a total of 23 tissues. The results were combined to create a labeled volume of the head with voxel dimensions of 0.33x0.33x0.33 mm. The individual label matrices and their corresponding surface meshes are made available to be used freely. The detailed blood vessel network and ocular tissues will be of interest in computational modelling and simulation studies.**

I. Introduction

The construction of anatomically detailed and accurate head models has been a constant endeavor among the modelling and simulation community. In brain studies, inverse imaging of brain activity needs very high resolution models of human brain and head [1]. Similarly, analysis of mobile phone specific absorption ratio (SAR) calculations in human head is an example of the need for high resolution human head models. For such applications, the accuracy and details of the head models plays an important role [1, 2]. However, in spite of available image data, labor intensive image segmentation due to lack of automatic tools have hindered the construction of such models. Moreover, the technological bottleneck in terms of computational power, has constrained the usability of these accurate models. Nonetheless, with ever-increasing hardware capabilities, the possibilities for modelling and simulation of physiological phenomena have also been expanding. Since the release of the Visible Human Project (VHP) data [3], there have been numerous efforts towards developing models with high accuracy - that is, in producing models of anatomies of increasing resolutions.

While developing general models, it is desirable to include as many pertinent tissues as possible with the highest achievable accuracy. There are two terms that need clarification when describing these models – details and accuracy. Detail refers to the number of anatomical tissues or objects that are present in the model, while accuracy refers to the degree of realism with which the tissues or objects are represented in the model. These two qualities are directly dependent on the image resolution since with increasing resolution it becomes possible to include more details with greater accuracy. Imaging resolutions limit the accuracy of models constructed through Magnetic Resonance Imaging (MRI) or Computed Tomography (CT) devices. However, the cryo-sectioning of Visible Human Male (VHM) produced data which was higher in resolution for documenting the human anatomy. Since the creation of VHM in 1994 there have been similar efforts in producing anatomical libraries in the highest detail such as Visible Human Female (VHF), Visible Korean human [4] and Visible Chinese human [5]. Correspondingly, there continues to be an active interest in creating segmented models of the head [6-9].

This paper describes procedures involved in creating a labeled, high resolution, isometric voxel model based on the VHF data, providing an accurate base for modeling tasks.

II. Material And Methods

A. Visible Human Female data

The Visible Human Projects' Female data was used as the source for all segmentations in this work. It consists of the MR, CT and anatomical cryo-section (here on referred to as "cryo") images of a 59 year old female donor. The choice of source data was dictated by the high image resolution, multiple image modalities, extensive documentation and ease of availability. While the CT and MR images were limited by the imaging equipment to clinical resolution standards, the cryo images were of higher resolution. In terms of voxel dimensions, the MR and CT images are of 0.94x0.94x1mm, while the cryo images are of 0.33x0.33x0.33mm. The original cryo data has 2048x1216x855 voxels, and being of a higher resolution, was used as the base for all subsequent work to maintain the high detail of the final result. More detailed information about the data and its acquisition can be found from Ackerman's paper [3].

The CT volume had a clear advantage in delineating the skull and other bone structures, and thus was used for the first segmentation task of obtaining the skull. We found that the MR data, due to its poor resolution, was not a good source for segmenting most major tissues. The T2-MR data, however, showed distinctly the presence of cerebrospinal fluid (CSF) and thus was used in its segmentation. All segmentations from CT and MR were interpolated to match the cryo resolution. Rigid registration with linear

Research supported by EMSOFT-project; Tekes (Finnish Funding Agency for Technology and Innovation) and Nokia and by The Finnish Cultural Foundation.

M. Hannula (phone: +358-40-8490025; e-mail: markus.hannula@tut.fi), N. Narra (e-mail: nathaniel.narragirish@tut.fi), N. Onnela (e-mail: niina.onnela@tut.fi) and J. Hyttinen (e-mail: jari.hyttinen@tut.fi) are with the Department of Electronics and Communications Engineering, Tampere University of Technology, P.O. Box 692, FI-33101 Tampere, Finland.

P. Dastidar is with the Medical Imaging Center, Tampere University Hospital, P.O. Box 2000, 33521 FI-Tampere, Finland (e-mail: prasun.dastidar@pshp.fi).

978-1-4244-7929-0/14/$26.00 ©2014 IEEE

interpolation was performed in order to merge segmentations from the CT and MR data sets with the segmentations from the cryo data.

The cryo images are RGB images where some tissue colors are biased towards one or two of the color channels. Thus, it was possible to choose the best of color channels or their arithmetic combinations, to enhance certain tissues to aid in their segmentation. For example, the background was extracted by subtracting the red from the blue channel, since the materials in which the subject was ensconced was blue in color. Eyes, blood and the brain were segmented from the red channel; muscles, fat and optic nerve from the green channel; and airways and sinuses were obtained from the blue channel.

B. Segmentation

In this work, we initially performed automatic segmentation using level sets and region growing methods in the initial phase. Wherever performance was deemed inadequate, we performed manual/semi-automatic segmentation using manual delineation, correction, adaptive thresholding and various morphological operators to maintain anatomical consistency. It especially became necessary in the extraction of cerebellum and ears; and in areas where fine tuning of the results was required. This can be attributed to the structural complexity of objects of interest, poor relative image quality of CT and MR data and registration errors. We found that the plane of imaging in the CT and the cryo data do not match perfectly. This was corrected by rotating the CT volume to realign with the axial plane of the cryo images.

Primary methods used in segmentation were thresholding [10], level sets [11], region growing [12] and morphological dilation and erosion operations [13]. Often several methods were used in combination for particular tissue segmentations. In broad terms, we applied thresholding for the extraction of skull, muscles and fat, level sets to segment gray and white matter and region growing with air ways and blood extraction. Parameters for these methods were selected with visual inspection. Morphological operations such as erosion and dilation were used in the creation of synthetic layers that were on the edge of the image resolution such as sub-layers of skin and eye. These in combination were used as closing and opening operations for correcting the results obtained from other segmentation methods. The segmentation of the various tissues was achieved in a sequential manner, where the result of the segmentation of one tissue was used in aiding the next. Thus, tissues such as skull and skin were segmented and when masked out from the data, tissues such as fat and muscle were more easily detected by the segmentation algorithms. As segmentation programs, Matlab (Math Works Inc., Natick, MA) was used with more advanced methods and ITK-snap (http://www.itksnap.org/) [14] with manual segmentation.

Segmentation was performed under the guidance of medical experts. In most cases, the segmented tissues were based on the image data. However when creating sub-layers for skin and eye, which were difficult to extract directly from the image data, established standard anatomical atlases were used as reference to create them artificially.

III. RESULTS

The result is a detailed segmentation of the human head based on the VHF data. The labelled model is represented by a matrix of dimensions 640x530x670, where each element is a voxel of isometric dimensions of 0.33 mm, resulting in over 120 million voxels that can be used for creating computational models. With the combined use of multiple image protocols we were able to obtain greater number of tissues with high accuracy.

In the segmented model there are 23 different tissue types listed in TABLE I.

TABLE I. SEGMENTED TISSUE TYPES AND THEIR VOLUMES

Tissue name	Volume (1000*mm3)
Brain	1343.56
Grey Matter	784.08
White Matter	416.49
Cerebellum	143.00
Eyes	16.13
Vitreous Humor	9.59
Lens	0.52
Anterior Chamber	0.20
Choroid	1.35
Cornea	0.26
Retina	1.26
Sclera	2.96
Skin	
Epidermis	54.27
Papillary Layer	53.33
Reticular Layer	157.77
Bone	627.77
Muscle	891.88
Air-Sinus	15.41
Cerebrospinal Fluid	137.43
Ear1	25.69
Ear2	25.59
Head Mix	939.16
Blood	19.20
Fat	309.88
Optic Nerve	1.36

Figure 1 presents three example visualizations of the segmented model. In the segmentation procedure, some tissues were segmented in more detail. The selection of the level of detail was based on the need for applications. E.g. for SAR-calculations of high frequency electromagnetic waves, eyes and skin are important.

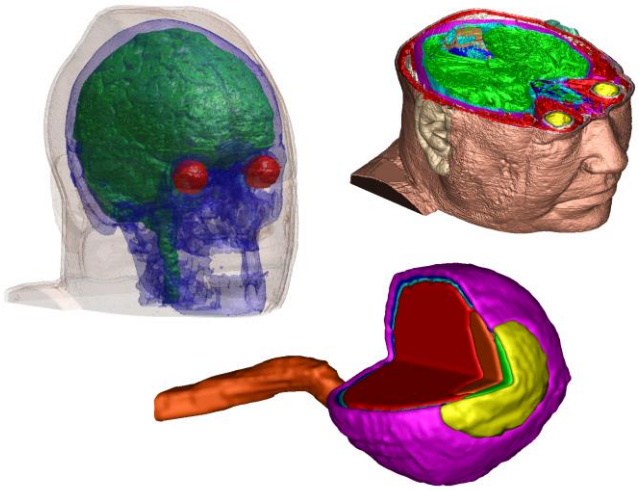

Figure 1. Two visualization of the head model with skull, brain, skin and eyes. In the third illustration there is an eyeball separated to different parts and an optic nerve.

Figure 2 illustrates the effect of resolution on the blood vessel network, where the continuity of the network deteriorates with decreasing resolution.

.

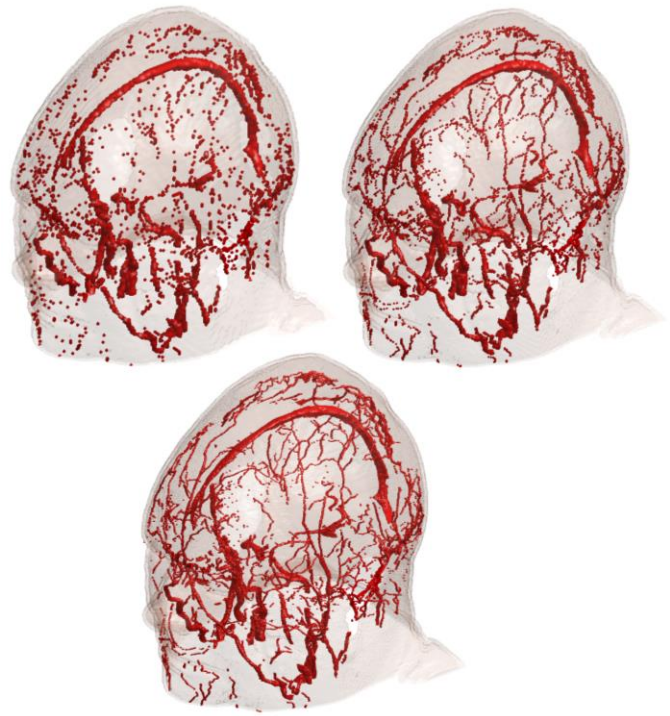

Figure 2. The effect of different voxel sizes – 1.5 mm (top left), 1 mm (top right) and 0.33 mm (bottom) on the continuity of the blood network.

IV. Discussion and Conclusion

This study presents a highly detailed, high resolution labeled volume of a human head based on the VHF data with 0.33 mm isometric voxels. This work was initiated for use in studying SAR and other bioelectric applications. Consequently the high level of details in the eye, skin and the significant blood network make this work particularly suitable for groups interested in modelling these tissues. The voxel data, as made available, can be directly used as voxel based mesh for finite difference models (FDM) [15]. In addition, the data can also be converted into volume meshes and used in computational analysis using finite element methods.

The VHF project as source data is attractive in many aspects as detailed in previous sections; however, it does present some difficulties. Since we used all three modalities (cryo, CT and MRI), we had to perform interpolation to match resolutions and registration to fit the data. This data registration task is further complicated by the fact that the MR and CT data stacks were obtained before freezing of the subject. This has introduced some noticeable deformations in the anatomy in the cryo images which are not always effectively corrected by registration. While this data is highly realistic, the images having been obtained post-mortem, will have certainly introduced slight variations in the tissue volumes and distribution, e.g. in the eyes and CSF distribution. However, the label model created in this work is adequate as a functional approximation for computational needs. For comparison, the Brain and eye volumes from International Commission on Radiological Protection (ICRP) reference woman data are 1250 ml and 14.6 ml respectively [16]. The corresponding volumes of the brain (1343 ml) and eyes (16.13 ml) in this work are within 10% of the ICRP's reference woman. In [4], Park et al. considered the elderly age and obese proportions of the subject as unrepresentative. While this argument does have merit, it may also be argued that our model can be used for the demography that is best represented by it – aged and slightly obese. In any case, using a single head model to represent every single person would be a serious generalization. Creating race specific head models would be a much more viable solution [17].

Segmentation algorithms, in terms of user interaction, range from completely manual to completely automatic. However, when dealing with objects which exhibit high complexity such as the human anatomy, it becomes prudent to either utilize semi-automatic methods or accomplish the task as a combination of automatic and manual phases. The segmentation algorithms implemented were applied over the 3D data stack. One important aspect of the model is that the segmentation procedure was not focused on an accurate voxel by voxel segmentation, but more on a general model creation. That is, by incorporating as much realism in the details as possible while not following each and every voxel in the data. Artificially created tissues, such as skin, are based on anatomical values and are equally thick throughout the head, which is not the case in reality but a close approximation. Wherever our semi-automated methods failed in producing reasonable results, the inaccuracies were corrected by manual segmentation.

In order to minimize errors due to the inaccuracy and peculiarities of the data, special care was taken during the segmentation procedure to maintain the realistic distribution of tissues that were at the edge of the resolution. Thus, the results of the segmentation algorithms were reviewed, corrected, and in some instances labels added in areas where anatomy dictated their presence. Example of such task is - ensuring the continuity of the ocular layers as a smooth surface, the blood network and demarcating epithelial layers of the skin. In certain application areas the increased resolution beyond 1mm adds minimal benefit in the usability of a model. However, it may be surmised that increased model resolution enhances the potential to study tissues which are at the edge of this measure. More accurate resolution should be used e.g. to model critical anatomies in bioelectric applications in areas where the conductivity is much higher than in surrounding tissues in general. As an example, the vasculature presented at different resolutions in Figure 2, clearly illustrates the benefit of increased resolution in representing a more complete blood network. This in turn increases the potential to model this important source of heat diffusion/transfer in high detail and study their role in applications such as studying SAR in tissues. High-resolution models will become even more useful with increasing computational resource availability and greater interest in processes within tissues of decreasing dimensions (or increasing resolution).

In the future, the labeled voxel data will be progressively converted into mesh files compatible with common FEA software programs. The collection of data and formats will make it possible to use this work as a base for tailoring it for specific needs in various applications. In its current form, it contains features that are suitable for many applications in SAR and EEG studies.

The result (labeled voxel volume) is made freely available to the public in the form of native MATLAB '.mat' files. www.biomeditech.fi/AnatomicalModels

REFERENCES

[1] K. Wendel, J. Väisänen, A. Kybartaite, J. Hyttinen and J. Malmivuo, "The significance of relative conductivity on thin layers in EEG sensitivity distributions," Biomedizinische Technik/Biomedical Engineering, vol. 55, pp. 123-131, 2010.

[2] P. Laarne, P. Kauppinen, J. Hyttinen, J. Malmivuo and H. Eskola, "Effects of tissue resistivities on electroencephalogram sensitivity distribution," Med Biol Eng Comput, vol. 37, pp. 555-559, 1999.

[3] M. Ackerman, "The visible human project," Proc IEEE, vol. 86, pp. 504-511, 1998.

[4] J. S. Park, M. S. Chung, S. B. Hwang, Y. S. Lee, D. H. Har and H. S. Park, "Visible Korean Human: Improved serially sectioned images of the entire body," IEEE Trans. Med. Imaging, vol. 24, pp. 352-360, 2005.

[5] S. X. Zhang, P. A. Heng, Z. J. Liu, L. W. Tan, M. G. Qiu, Q. Y. Li, R. X. Liao, K. Li, G. Y. Cui and Y. L. Guo, "Creation of the Chinese visible human data set," Anat. Rec., vol. 275, pp. 190-195, 2003.

[6] C. H. Wolters, A. Anwander, X. Tricoche, D. Weinstein, M. A. Koch and R. S. MacLeod, "Influence of tissue conductivity anisotropy on EEG/MEG field and return current computation in a realistic head model: a simulation and visualization study using high-resolution finite element modeling," Neuroimage, vol. 30, pp. 813-826, 2006.

[7] A. Christ, W. Kainz, E. G. Hahn, K. Honegger, M. Zefferer, E. Neufeld, W. Rascher, R. Janka, W. Bautz and J. Chen, "The Virtual Family—development of surface-based anatomical models of two adults and two children for dosimetric simulations," Phys. Med. Biol., vol. 55, pp. N23, 2010.

[8] M. Halko, A. Datta, E. Plow, J. Scaturro, M. Bikson and L. Merabet, "Neuroplastic changes following rehabilitative training correlate with regional electrical field induced with tDCS," Neuroimage, vol. 57, pp. 885-891, 2011.

[9] W. H. Lee and T. Kim, "Methods for high-resolution anisotropic finite element modeling of the human head: Automatic MR white matter anisotropy-adaptive mesh generation," Med. Eng. Phys., vol. 34, pp. 85-98, 2012.

[10] M. Sezgin and B. Sankur, "Survey over image thresholding techniques and quantitative performance evaluation," J. Electron. Imaging, vol. 13, pp. 146-168, 2004.

[11] J. A. Sethian, "Level set methods and fast marching methods," J. Computing Inf. Technol., vol. 11, pp. 1-2, 2003.

[12] R. Adams and L. Bischof, "Seeded region growing," IEEE Trans. Pattern Anal. Mach. Intell., vol. 16, pp. 641-647, 2002.

[13] F. Meyer and S. Beucher, "Morphological segmentation," J Vis Commun Image R, vol. 1, pp. 21-46, 1990.

[14] P. A. Yushkevich, J. Piven, H. C. Hazlett, R. G. Smith, S. Ho, J. C. Gee and G. Gerig, "User-guided 3D active contour segmentation of anatomical structures: significantly improved efficiency and reliability," Neuroimage, vol. 31, pp. 1116-1128, 2006.

[15] P. Kauppinen, J. Hyttinen, P. Laarne and J. Malmivuo, "A software implementation for detailed volume conductor modelling in electrophysiology using finite difference method," Comput. Methods Programs Biomed., vol. 58, pp. 191-203, 1999.

[16] J. Valentin, Basic Anatomical and Physiological Data for use in Radiological Protection: Reference Values. Elsevier Science Health Science div, 2003.

[17] K. Wendel, "The influence of tissue conductivity and head geometry on EEG measurement sensitivity distributions," Tampere University of Technology. Doctoral Dissertation., vol. 900, pp. 62, [52] p, 2010.